

Supporting Information

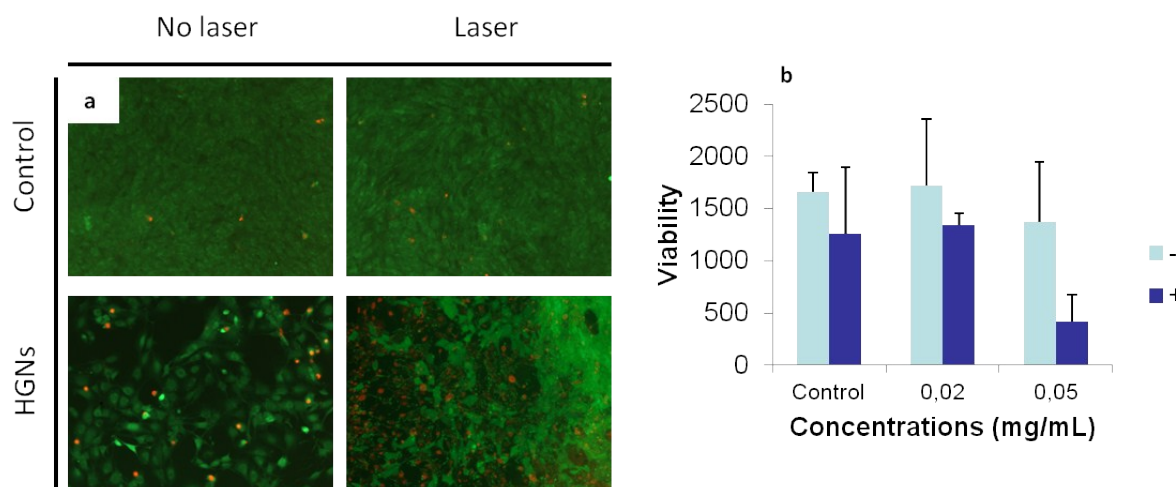
Selective Delivery of Photothermal Nanoparticles to Tumors Using Mesenchymal Stem Cells as Trojan Horses

M. Mar Encabo-Berzosa^{a,b,c}, Marina Gimeno^d, Lluís Lujan^d, Maria Sancho-Albero^{a,b}, Leyre Gomez^{a,b}, Victor Sebastian^{a,b}, Miguel Quintanilla^e, Manuel Arruebo^{a,b, §}, Jesus Santamaria^{a,b}, Pilar Martin-Duque^{c,f,g§}

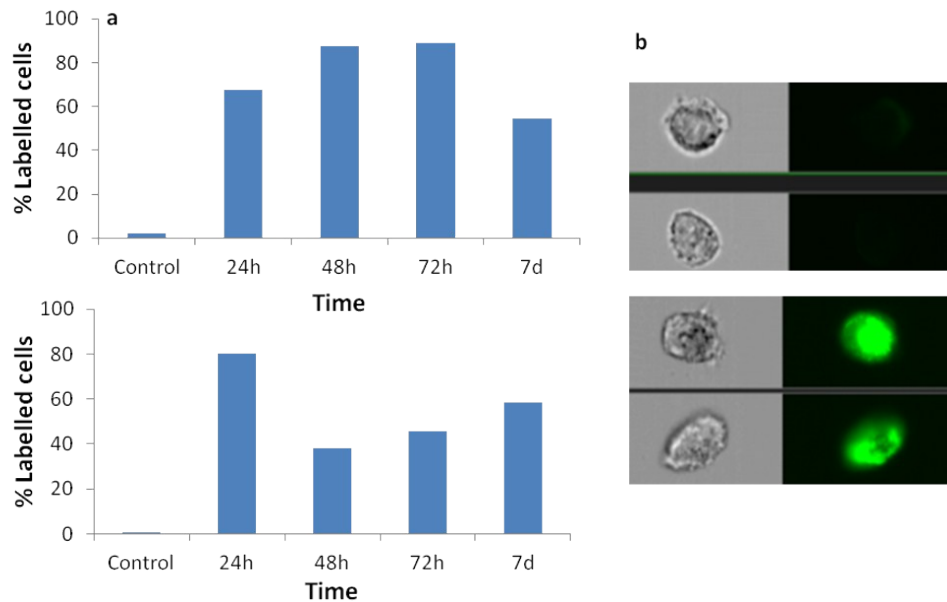
Cell irradiation

To distinguish the cell death pathways a LIVE/DEAD test was performed. When cells carrying HGNs were irradiated, the nanoparticle photothermal induced effect was observed and cell death initiated. On cells undergoing apoptosis, damage occurs mainly in the membrane (**Supplementary Figure 1**), allowing the entry of the ethidium homodimer, staining the nucleus in red. In the case of the viable cells, i.e. not damaged, the cell membrane is stained with calcein (green). The number of damaged cells (red nucleus) was compared with and without laser irradiation and with and without HGNs, resulting in a superior cell reduction when using HGNs and laser irradiation (**Supplementary Figure 1a**). So, we can conclude that when the HGNs are irradiated with NIR laser, they mediate protein denaturalization and consequent cell death. The same conclusion can be drawn from the viability test results by AlamarBlue (**Supplementary Figure 1b**). Neither the laser irradiation in the absence of HGNs or nanoparticles in absence of laser were capable to cause cell-damage.

Supplementary Figure 1. (a) LIVE/DEAD[®] test results. The fluorescent reagents of the kit stained the cell membranes in green and the nuclei in red, being labeled in red when cell damage was induced. A lower number of damaged cells in the controls and in the MSCs only with HGNs were observed. A stronger red labeling is shown when the cells with internalized HGNs were irradiated. (b) Alamar Blue assay: In all cases the cells without irradiation (-) showed higher viability than cells with NIR laser irradiation (+). Cell viability decreased in a dose dependent manner after HGNs addition. The differences were statistically significant ($P < 0.05$).



Supplementary Figure 2. Flow cytometry based kinetics of the internalization process (a) Nanoparticle internalization kinetics of HGNs (top) and PEG-HGNs (bottom) presented as percentage of total MSCs containing HGNs at different times after incubation. (b) Image of the flow cytometer showing control cells (top) and rhodamine labelled gold nanoparticles loaded within MSCs (bottom).



HGNs active internalization

In order to study the internalization profile of the HGNs within MSCs a live cell imaging was performed. MSCs were incubated with $50 \mu\text{g}\cdot\text{mL}^{-1}$ during 72 h and during this time they were maintained at 37°C in a 5% CO_2 -humidified atmosphere in an incubator coupled to a multidimensional microscope with real-time control Leica AF6000 LX. Active HGNs cellular internalization and exocytosis was observed during this time.

Supplementary Figure 3. Photographs of the video showing the dynamic internalization process. A nanoparticle contained within a cell is exocytosed to the extracellular space and then another cell uptakes the same nanoparticle.

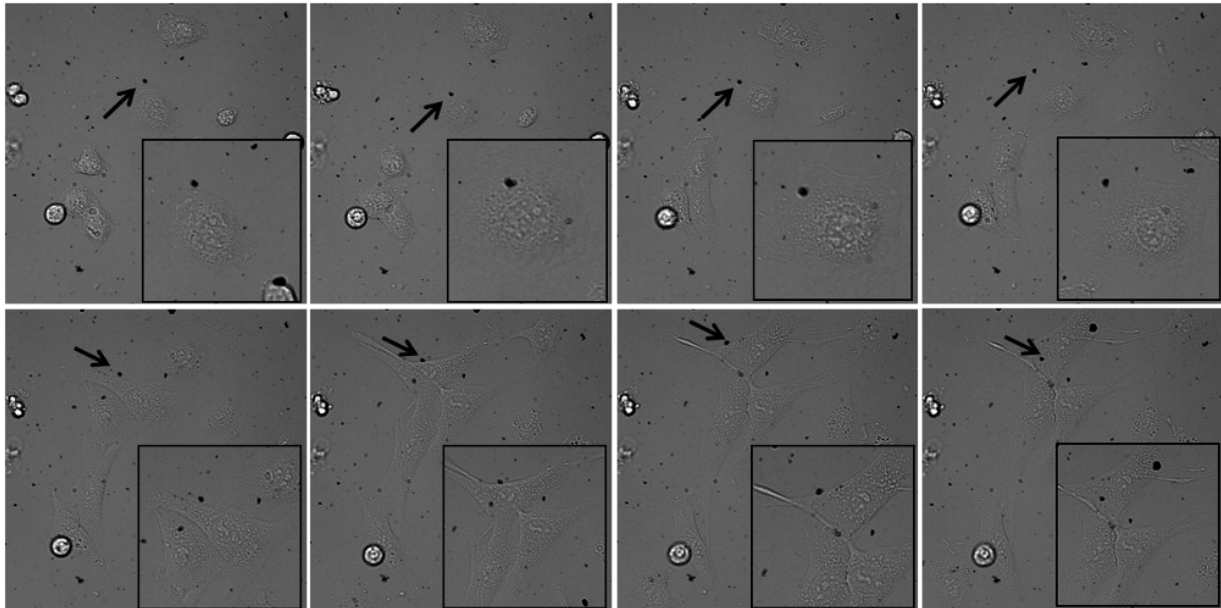


Table 1. Immunohistochemical staining for Ki-67 expression on tumor cells

Groups	% Ki67 positive cells	% Ki67 negative cells
Control (B1)	78	22
PEG-HGNs+ laser (B2)	66	34
MSC + PEG-HGN + laser (B3)	59	41
MSCs+ PEG-HGNs (B4)	76	24